Identification of a New Form of Electron Coupling in the $Bi_2Sr_2CaCu_2O_8$ Superconductor by Laser-Based Angle-Resolved Photoemission Spectroscopy

Wentao Zhang,[1] Guodong Liu,[1] Lin Zhao,[1] Haiyun Liu,[1] Jianqiao Meng,[1] Xiaoli Dong,[1] Wei Lu,[1] J. S. Wen,[2] Z. J. Xu,[2] G. D. Gu,[2] T. Sasagawa,[3] Guiling Wang,[4] Yong Zhu,[5] Hongbo Zhang,[4] Yong Zhou,[4] Xiaoyang Wang,[5] Zhongxian Zhao,[1] Chuangtian Chen,[5] Zuyan Xu,[4] and X. J. Zhou[1,*]

[1] *National Laboratory for Superconductivity, Beijing National Laboratory for Condensed Matter Physics, Institute of Physics, Chinese Academy of Sciences, Beijing 100080, China*

[2] *Condensed Matter Physics and Materials Science Department, Brookhaven National Laboratory, Upton, New York 11973, USA*

[3] *Materials and Structures Laboratory, Tokyo Institute of Technology, Yokohama Kanagawa, Japan*

[4] *Laboratory for Optics, Beijing National Laboratory for Condensed Matter Physics, Institute of Physics, Chinese Academy of Sciences, Beijing 100080, China*

[5] *Technical Institute of Physics and Chemistry, Chinese Academy of Sciences, Beijing 100080, China*

(Received 19 December 2007; published 14 March 2008)

Laser-based angle-resolved photoemission measurements with superhigh resolution have been carried out on an optimally doped $Bi_2Sr_2CaCu_2O_8$ high temperature superconductor. New high energy features at ~115 meV and ~150 meV, in addition to the prominent ~70 meV one, are found to develop in the nodal electron self-energy in the superconducting state. These high energy features, which cannot be attributed to electron coupling with single phonon or magnetic resonance mode, point to the existence of a new form of electron coupling in high temperature superconductors.

DOI: 10.1103/PhysRevLett.100.107002 PACS numbers: 74.72.Hs, 71.38.−k, 74.25.Jb, 79.60.−i

The physical properties of materials are dictated by the microscopic electron dynamics that relies on the many-body effects, i.e., the interactions of electrons with other excitations, such as phonons, magnons, and so on. How to detect and disentangle these many-body effects is critical to understanding the macroscopic physical properties and the superconductivity mechanism in high temperature superconductors. Angle-resolved photoemission spectroscopy (ARPES), as a powerful tool in probing many-body effects [1], has revealed clear evidence of electron coupling with low-energy collective excitations (bosons) at an energy scale of ~70 meV [2–7] in the nodal region and ~40 meV near the antinodal region [4,8–10] although the nature of the bosonic modes remains under debate as to whether it is phonon [5,6,10] or magnetic resonance mode [3,4,7,8,11]. Recently, another high energy feature has been identified in dispersion at 300–400 meV, but its origin remains unclear as to whether this can be attributed to a many-body effect [12].

In this Letter we report an identification of a new form of electron coupling in high temperature superconductors by taking advantage of a superhigh resolution vacuum ultraviolet (VUV) laser-based ARPES technique [13]. New features at energy scales of ~115 meV and ~150 meV are revealed in the electron self-energy in the $Bi_2Sr_2CaCu_2O_8$ (Bi2212) superconductor in the superconducting state. These features cannot be attributed to electron coupling with single phonon mode or magnetic resonance mode. They point to a possibility of electron coupling with some high energy excitations in high temperature superconductors.

The angle-resolved photoemission measurements have been carried out on our newly developed VUV laser-based angle-resolved photoemission system [13]. The photon energy of the laser is 6.994 eV with a bandwidth of 0.26 meV. The energy resolution of the electron energy analyzer (Scienta R4000) is set at 0.5 meV, giving rise to an overall energy resolution of 0.56 meV, which is significantly improved from 10–15 meV from regular synchrotron radiation systems [2–7]. The angular resolution is ~0.3°, corresponding to a momentum resolution ~0.004 $Å^{-1}$ at the photon energy of 6.994 eV, more than twice improved from 0.009 $Å^{-1}$ at a regular photon energy of 21.2 eV for the same angular resolution. The photon flux is adjusted between 10^{13} and 10^{14} photons/second. The optimally doped Bi2212 single crystals with a superconducting transition temperature $T_c = 91$ K were cleaved *in situ* in vacuum with a base pressure better than 5×10^{-11} Torr.

Figure 1(a) shows the raw data of photoelectron intensity as a function of energy and momentum for an optimally doped Bi2212 superconductor ($T_c = 91$ K) measured along the $\Gamma(0,0) - Y(\pi,\pi)$ nodal direction at a temperature of 17 K. By fitting momentum distribution curves (MDCs), the dispersion [Fig. 1(b)] and MDC width [inset of Fig. 1(b)] are quantitatively extracted from Fig. 1(a). One can see an obvious kink in dispersion near 70 meV [Figs. 1(a) and 1(b)] and a drop in the MDC width [inset of Fig. 1(b)], similar to those reported before [2–7] but with much improved clarity. It is generally agreed that this 70 meV feature originates from a coupling of electrons with a collective boson mode. When coming to the nature of the boson mode, it remains under debate whether it is phonon [5,6] or magnetic resonance mode [3,4,7].

The real part of the electron self-energy can be extracted from the dispersion given that the bare band dispersion is

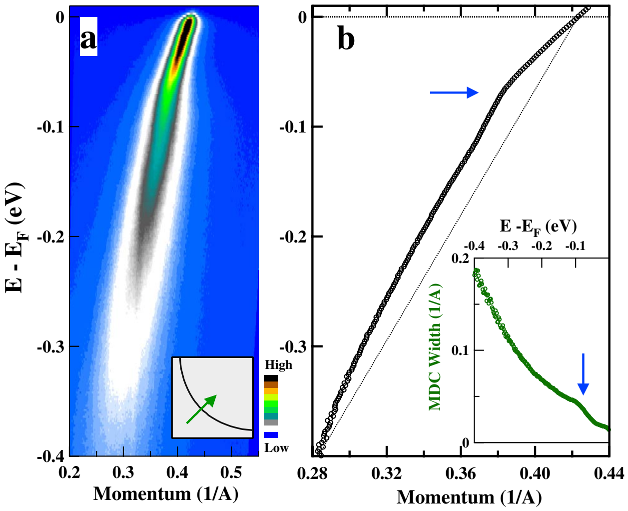

FIG. 1 (color online). Electron dynamics of optimally doped Bi2212 ($T_c = 91$ K) measured along the $\Gamma(0,0) - Y(\pi,\pi)$ nodal direction at 17 K. (a) Raw image showing photoelectron intensity (represented by false color) as a function of energy and momentum. The inset shows the location of the momentum cut in the Brillouin zone; (b) nodal dispersion extracted from (a) by fitting MDCs. The dotted line connecting the two energy positions in the dispersion at the Fermi energy and -0.4 eV is an empirical bare band for extracting the effective real part of self-energy in Fig. 2(b). The inset shows the corresponding MDC width (FWHM).

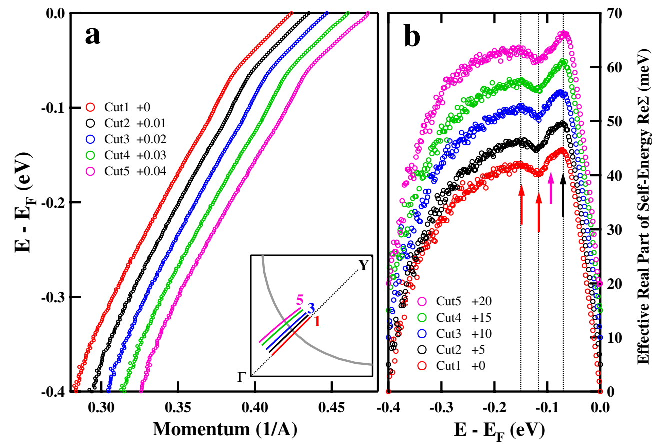

FIG. 2 (color online). Momentum dependence of dispersions (a) and corresponding effective real part of electron self-energy (b). The inset of (a) shows the location of momentum cuts in the Brillouin zone. The effective self-energy in (b) is obtained by taking the straight line connecting two positions in dispersion at the Fermi energy and -0.4 eV as a bare band. The arrows in (b) mark fine features at $\sim$70 meV, 115 meV, and 150 meV, and a possible feature near 94 meV. For clarity, curves in (a) are offset along the momentum axis, while curves in (b) are offset along the vertical axis; the offset values are given in the legends.

known which can be determined in a number of ways but still without consensus [14,15]. To identify fine features in the electron self-energy and study their relative change with temperature, it is reasonable to assume a featureless bare band for the nodal dispersion within a small energy window near the Fermi energy. In this case, the fine features manifest themselves either as peaks or curvature changes in the "effective self-energy"[15]. As shown in Fig. 1(b), we choose here a straight line connecting two energy positions in the dispersion at the Fermi energy and -0.4 eV as the empirical bare band. The resultant effective real part of electron self-energy, which represents the energy difference between the measured dispersion and the selected bare band, is shown in Fig. 2(b). Also shown in Fig. 2 are dispersions [Fig. 2(a)] along several other cuts in the Brillouin zone [inset of Fig. 2(a)] and the corresponding effective electron self-energy [Fig. 2(b)].

With much improved precision of data, one can identify clearly several features in the electron self-energy, as shown in Fig. 2(b). The most pronounced feature is the peak at $\sim$70 meV that gives rise to the kink in dispersion seen here and before [2–7]. In addition, at higher energies, two new features can be identified clearly as a valley at $\sim$115 meV and a cusp at $\sim$150 meV. The signature of a fine feature near 94 meV is also visible, particularly for the two cuts close to the nodal region (cuts 1 and 2). Between the Fermi level and 70 meV, we have also observed hints of possible low-energy features which are, however, very subtle and need further measurements to pin them down. We note that the bare band selection has little effect on the identification of these fine features and their energy position as we have checked by trying other straight lines as empirical bare bands. Particularly, the two new features at 115 meV and 150 meV, together with the 70 meV peak, are robust (as also shown in Fig. 4 below) and persist in a rather large momentum space near the nodal region.

The nodal electron dynamics undergoes a dramatic evolution with temperature and superconducting transition, as indicated by the temperature dependence of the nodal dispersion [Fig. 3(a)] and scattering rate [Fig. 3(b)]. In Fig. 3(a), a quantitative momentum variation with temperature at four typical energy positions (the Fermi level, -0.07 eV, -0.2 eV, and -0.3 eV) is plotted in the upper-left inset, and some representative MDCs for these four energies at 17 K and 128 K are plotted in the bottom-right inset. Over the temperature range of the measurement, the dispersion change with temperature spreads over an energy range of 0–300 meV within which the dispersion renormalization gets stronger with decreasing temperature.

An unexpected finding is the Fermi momentum shift with temperature [Fig. 3(a) and top-left inset], which increases with increasing temperature in the superconducting state below $T_c = 91$ K and then becomes nearly flat above T_c. The magnitude of the shift is small, on the order of 0.003 Å^{-1}, and the change is monotonic. We first checked whether this could be caused by a sample orientation change during the heating or cooling process and feel that it is unlikely because this usually would cause a shift of overall dispersion. As shown in Fig. 3(a) and the top-left inset, the dispersion above 300 meV shows little change

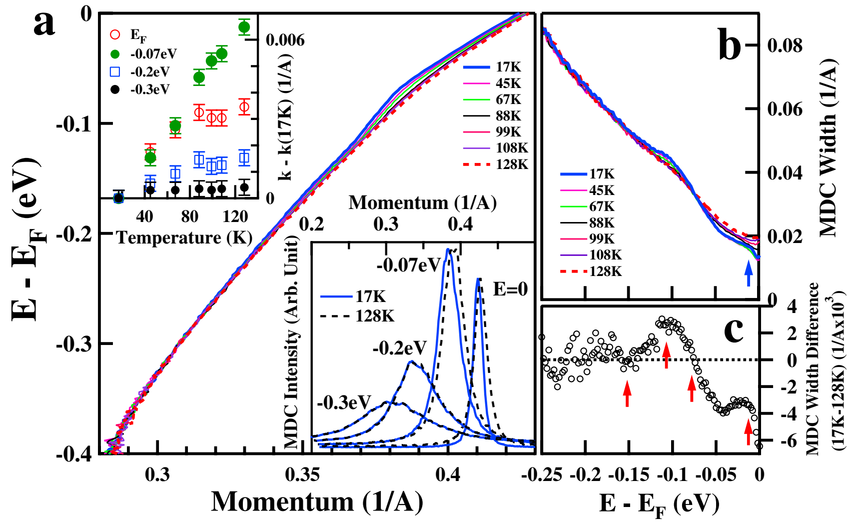

FIG. 3 (color online). Temperature dependence of the nodal MDC dispersion (a) and MDC width (b). The top-left inset of (a) plots the momentum value as a function of temperature at four typical energies: E_F [empty (red) circle], -0.07 eV [solid (green) circle], -0.2 eV [empty (blue) square], and -0.3 eV [solid (black) circle] obtained by averaging over the ± 10 meV energy range. The bottom-right inset of (a) shows MDCs at these four energies measured at 17 K (solid line) and 128 K (dashed line). (c) The difference of the MDC width between two temperatures at 17 K and 128 K. The arrows in (b) and (c) mark possible features showing up in the scattering rate.

with temperature. In fact, the MDCs themselves at 300 meV overlap with each other at 17 K and 128 K almost perfectly, as shown in the bottom-right inset of Fig. 3(a). Another possibility we have checked is whether it can be caused by the thermal expansion or contraction of the sample during temperature change. This can also be excluded because with the lattice expansion with increasing temperature, one would expect a shrink of the Brillouin zone that causes the nodal Fermi momentum move to a smaller value; this expected trend is just the opposite to our experimental observation. Because the Fermi momentum shift with temperature is quite unusual and has not been reported before, we have repeated the measurement and reproduced the similar observation. Therefore, to the best of our efforts, we think this is likely an intrinsic effect and its first observation is a result of much improved instrumental precision. Further work needs to be done to pin down this effect and understand the underlying physical origin as it suggests either a chemical potential shift or Fermi surface topology change upon entering the superconducting state.

The scattering rate shows a strong variation with temperature at the low-energy range within 0 to -0.2 eV, as shown in Fig. 3(b). Interestingly, the temperature dependence is not monotonic but depends on the binding energy. Between the Fermi level and -0.07 eV, the scattering rate decreases with decreasing temperature, while it increases with decreasing temperature between -0.07 and -0.15 eV. This gives rise to an "overshoot" region extending to ~ -0.1 eV at low temperature. The change of the scattering rate with temperature can also be clearly seen in the difference between the normal and superconducting states, as plotted in Fig. 3(c) which depicts the difference between 17 K and 128 K data. Here the difference between -0.07 eV and -0.15 eV is positive while it becomes negative between E_F and -0.07 eV.

The temperature dependence of the effective real part of self-energy (Fig. 4) indicates that the new high energy features at 115 meV and 150 meV are developed in the superconducting state. Figure 4(a) shows the effective real part of self-energy at various temperatures obtained from the dispersions [Fig. 3(a)] by selecting a common empirical bare band, i.e., a straight line connecting the Fermi energy and -0.4 eV in the dispersion at 128 K. Figure 4(b) shows the net temperature change of electron self-energy with respect to the normal state data at 128 K, thus avoiding any ambiguity from bare band selection. It is clear in both cases that a dramatic change of electron self-energy occurs in the superconducting state, with a sharpening of the $\sim$70 meV feature, together with the emerging and growing of the $\sim$115 meV and $\sim$150 meV features. These observations are consistent with the scattering rate data where one can see the emergence of similar characteristic energy scales at $\sim$150 meV, $\sim$115 meV, and $\sim$70 meV in the superconducting state [Fig. 3(c)].

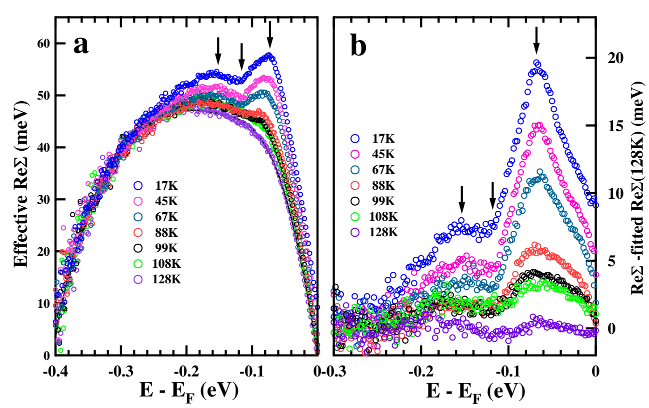

FIG. 4 (color online). (a) Temperature dependence of the effective real part of electron self-energy extracted from dispersions in Fig. 3(a) by taking a straight line as a bare band connecting two points at E_F and -0.4 eV on the dispersion at 128 K. (b) Temperature dependence of the difference between the measured self-energy in (a) and the fitted one for 128 K [solid black line in (a)]. The 128 K self-energy is fitted by polynomials and used to reduce statistical errors.

The identification of high energy features at 115 meV and 150 meV points to a new form of electron coupling in high temperature superconductors. These are qualitatively different from the ~70 meV feature which is attributed to coupling of electrons with some collective modes, and such modes with comparable energy scales are available in high temperature superconductors either as phonon [5,6] or magnetic resonance mode [3,4,7]. Because the energy scale of these two new features is higher than the maximum energy of phonons (~90 meV) [16] and the magnetic resonance mode (42 meV in optimally doped Bi2212) [17], they cannot be due to electron coupling with a single phonon or magnetic resonance mode. Although the effect of the electron-boson coupling for a low-energy mode can extend to high energy in the electron self-energy, it will not generate any new features with clear curvature change, as evidenced from simulations of electron-phonon coupling using both Debye and Einstein models and confirmed in canonical electron-phonon coupling systems [18].

There are a couple of possibilities that may give rise to high energy features in the electron coupling. The first is the mode energy shift due to the opening of superconducting gap: the original mode position in the normal state is expected to be shifted upward by an amount on the order of the superconducting gap upon entering the superconducting state [19]. In the optimally doped Bi2212, with the maximum *d*-wave superconducting gap at ~35 meV, one might expect that the original ~70 meV mode be shifted to a higher energy around 105 meV. However, this scenario is difficult to explain the existence of another 150 meV feature, the feature at 110 meV being a valley instead of a peak and the remaining strong ~70 meV feature. Another possibility is the electron coupling with multiple phonons. Usually this effect is expected to be much weaker [20] although, in principle, the possibility cannot be totally excluded. More theoretical work is needed to verify whether such a multiphonon process can produce clear features at high energy and whether such an effect is enhanced at low temperature. The third possibility is electron coupling with excitations that are already present at such high energy scales. The emergence and evolution of the 115 meV and 150 meV features in the electron self-energy is probably due to the redistribution of the underlying spectral function of the high energy excitations with temperature and superconducting transition. One candidate of such high energy excitations in high temperature superconductors seems to be naturally related to the spin fluctuation observed by neutron scattering, which covers a large energy range up to 200 meV and exhibits strong temperature dependence [21]. The signature of such high energy coupling is also proposed from optical measurements [22]. Further theoretical work to investigate the effect of such high energy spin excitations on electron dynamics will help in clarifying such a scenario.

In conclusion, by performing high precision ARPES measurements on Bi2212, we have revealed new features at 115 meV and 150 meV in the electron self-energy developed in the superconducting state. They cannot be attributed to electron coupling with either the single phonon or magnetic resonance mode, but point to the existence of a new form of electron coupling in high temperature superconductors. We hope this observation will stimulate further theoretical work to understand their origin and their role in determining anomalous physical properties of high temperature superconductors.

We acknowledge helpful discussions with J. R. Shi, T. Xiang, Z. Y. Weng, and S. Kivelson. This work is supported by the NSFC, the MOST of China (973 project Nos. 2006CB601002, 2006CB921302), and CAS (Projects ITSNEM and 100-Talent). The work at BNL is supported by the DOE under Contract No. DE-AC02-98CH10886.

*Corresponding author.
XJZhou@aphy.iphy.ac.cn

[1] A. Damascelli *et al.*, Rev. Mod. Phys. **75**, 473 (2003); J. C. Campuzano *et al.*, in *The Physics of Superconductors*, edited by K. H. Bennemann and J. B. Ketterson (Springer, New York, 2004), Vol. 2; X. J. Zhou *et al.*, in *Handbook of High-Temperature Superconductivity: Theory and Experiment*, edited by J. R. Schrieffer (Springer, New York, 2007).
[2] P. V. Bogdanov *et al.*, Phys. Rev. Lett. **85**, 2581 (2000).
[3] P. Johnson *et al.*, Phys. Rev. Lett. **87**, 177007 (2001).
[4] A. Kaminski *et al.*, Phys. Rev. Lett. **86**, 1070 (2001).
[5] A. Lanzara *et al.*, Nature (London) **412**, 510 (2001).
[6] X. J. Zhou *et al.*, Nature (London) **423**, 398 (2003).
[7] A. A. Kordyuk *et al.*, Phys. Rev. Lett. **97**, 017002 (2006).
[8] A. D. Gromko *et al.*, Phys. Rev. B **68**, 174520 (2003).
[9] T. K. Kim *et al.*, Phys. Rev. Lett. **91**, 167002 (2003).
[10] T. Cuk *et al.*, Phys. Rev. Lett. **93**, 117003 (2004).
[11] M. Eschrig and M. R. Norman, Phys. Rev. Lett. **85**, 3261 (2000).
[12] F. Ronning *et al.*, Phys. Rev. B **71**, 094518 (2005); J. Graf *et al.*, Phys. Rev. Lett. **98**, 067004 (2007); B. P. Xie *et al.*, Phys. Rev. Lett. **98**, 147001 (2007); T. Valla *et al.*, Phys. Rev. Lett. **98**, 167003 (2007); W. Meevasana *et al.*, Phys. Rev. B **75**, 174506 (2007); J. Chang *et al.*, Phys. Rev. B **75**, 224508 (2007); D. S. Inosov *et al.*, Phys. Rev. Lett. **99**, 237002 (2007).
[13] G. D. Liu *et al.*, Rev. Sci. Instrum. **79**, 023105 (2008).
[14] A. A. Kordyuk *et al.*, Phys. Rev. B **71**, 214513 (2005).
[15] X. J. Zhou *et al.*, Phys. Rev. Lett. **95**, 117001 (2005).
[16] R. J. McQueeney *et al.*, Phys. Rev. Lett. **87**, 077001 (2001).
[17] H. He *et al.*, Phys. Rev. Lett. **86**, 1610 (2001).
[18] M. Hengsberger *et al.*, Phys. Rev. B **60**, 10 796 (1999).
[19] A. W. Sandvik *et al.*, Phys. Rev. B **69**, 094523 (2004).
[20] S. Engelsberg and J. R. Schrieffer, Phys. Rev. **131**, 993 (1963).
[21] H. F. Fong *et al.*, Phys. Rev. B **61**, 14 773 (2000); P.-C. Dai *et al.*, Science **284**, 1344 (1999); B. Vignolle *et al.*, Nature Phys. **3**, 163 (2007).
[22] J. Hwang *et al.*, Phys. Rev. B **75**, 144508 (2007).